Forward kinematics of a general Stewart–Gough platform by elimination templates

Evgeniy Martyushev

Institute of Natural Sciences and Mathematics, South Ural State University, 76 Lenin Avenue, Chelyabinsk 454080, Russia
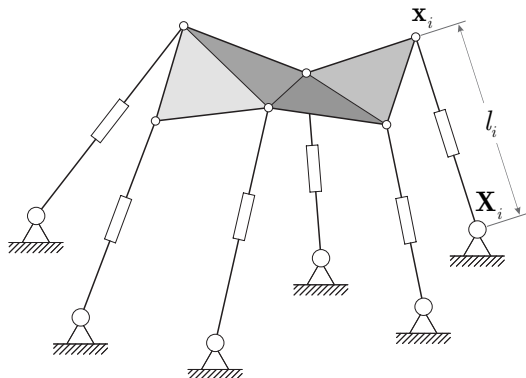
ABSTRACT

The paper proposes an efficient algebraic solution to the problem of forward kinematics for a general Stewart–Gough platform. The problem involves determining all possible postures of a mobile platform connected to a fixed base by six legs, given the leg lengths and the internal geometries of the platform and base. The problem is known to have 40 solutions (whether real or complex). The proposed algorithm consists of three main steps: (i) a specific sparse matrix of size 293×362 (the elimination template) is constructed from the coefficients of the polynomial system describing the platform's kinematics; (ii) the PLU decomposition of this matrix is used to construct a pair of 69×69 matrices; (iii) all 40 solutions (including complex ones) are obtained by computing the generalized eigenvectors of this matrix pair. The proposed algorithm is numerically robust, computationally efficient, and straightforward to implement — requiring only standard linear algebra decompositions. MATLAB, Julia, and Python implementations of the algorithm will be made publicly available.

1. Introduction

A Stewart–Gough platform (SGP) is a parallel manipulator widely used in applications such as flight simulators, robotic manipulators, haptic devices, surgical robots, radio telescopes, etc. It consists of a fixed base and a movable platform linked by six independently extensible legs. Each leg is attached to both the base and the platform via spherical joints, allowing for a wide range of motion, see Figure 1. The leg lengths are typically adjusted using actuators — such as hydraulic or pneumatic cylinders — allowing precise control over the platform's position and orientation [9, 41].


Figure 1: A general Stewart–Gough platform: both the base and top platform may be non-planar and asymmetric

The general SGP makes no assumptions about planarity or symmetry in either the fixed base or movable platform. This fully parallel mechanism has six degrees of freedom, meaning it can move in three translational directions and three rotational directions (pitch, roll, yaw). This allows the platform to move freely in 3-dimensional space.

The forward (or direct) kinematics problem for a Stewart–Gough platform involves determining the position and orientation of the movable platform given the lengths of the six extensible legs and the internal geometries of the

✉ martiushevev@susu.ru (Martyushev)
ORCID(s): 0000-0002-6892-079X (Martyushev)

platform and base. This problem is inherently complex due to the parallel structure of the platform, resulting in a system of non-linear polynomial equations. It has been shown that the problem has exactly 40 solutions in complex space [35, 22, 30, 43].

Since the early 1990s, many approaches have been developed to address the forward kinematics problem for a general SGP. Some of them include the use of Newton–Raphson and Levenberg–Marquardt algorithms for local refinement [27, 44, 11]; polynomial resultant theory and Gröbner bases [14, 23, 24, 12, 31]; interval analysis [6, 28]; metaheuristic optimization strategies, such as genetic algorithms [2, 40, 33] and particle swarm optimization [45]; precomputed lookup tables [42]; machine learning techniques, such as neural networks [36, 34, 4] and regression [29]. Each approach has its own strengths and limitations, see survey [37] for a description and comparison of some of the methods.

In addition to general approaches, specialized methods have been developed for SGPs with specific geometric configurations or augmented sensing capabilities. These approaches exploit simplified kinematics from symmetric or planar base/platform designs [10, 15, 32, 16, 13], additional sensor data to reduce solution space [38, 39, 17]. Such adaptations often yield closed-form solutions or order-of-magnitude speed improvements compared to general-case algorithms.

While substantial progress has been made in developing forward kinematics solvers for a general SGP, achieving an optimal balance between computational efficiency, numerical accuracy, and implementation simplicity remains an open fundamental challenge in parallel robotics. This paper addresses this challenge through a novel algebraic solver based on the method of elimination templates. This method, widely adopted in computer vision for minimal problems since the late 2000s [19, 20, 21, 1, 26, 25], provides the following advantages for the problem of forward kinematics:

- computation of all 40 solutions (real and complex);

- simultaneous maintenance of numerical accuracy and computational efficiency;

- reliance on standard linear algebra decompositions (PLU and QZ);

- extension to two special SGP cases without modification (Section 5).

The rest of the paper is organized as follows. Section 2 briefly introduces the method of elimination templates for solving 0-dimensional systems of polynomial equations. Section 3 formulates the forward kinematics problem as a system of six polynomial equations. Section 4 details the proposed elimination template based algorithm for solving the forward kinematics problem for a general SGP. Section 5 validates the solver in a series of experiments on synthetic data, evaluating in particular the numerical accuracy and computational performance of the solver. Finally, Section 6 discusses the results of the paper. For complete reproducibility, the Appendix includes all necessary data required to construct the elimination template.

2. Elimination templates

In this section we briefly recall the method of elimination templates for efficiently finding roots of 0-dimensional polynomial systems, see [19, 3, 20, 21, 1, 26, 25] for details.

Let $X = \{x_1, \dots, x_k\}$ be a set of k variables, $\mathbb{C}[X]$ the polynomial ring over the complex field $\mathbb{C}$, and

$$U = \{x_1^{\alpha_1} \dots x_k^{\alpha_k} \ : \ \alpha_i \in \mathbb{Z}_+\} \tag{1}$$

the set of monomials in X. We denote by $\mathbf{v}(\mathcal{A})$ the vector consisting of the elements of a finite set of monomials $\mathcal{A} \subset U$ which are ordered according to a certain total ordering on U.

Given a polynomial $f \in \mathbb{C}[X]$, we denote by U_f the support of f, i.e.,

$$U_f = \{m \in U \ : \ c(f, m) \neq 0\}, \tag{2}$$

where $c(f, m)$ is the coefficient of f at monomial m. Given a set of polynomials $F = \{f_1, \dots, f_s\} \subset \mathbb{C}[X]$, we denote by U_F the support of F, that is

$$U_F = \bigcup_{i=1}^{s} U_{f_i}. \tag{3}$$

Let $n = \#U_F$ be the cardinality of the finite set U_F. The *Macaulay matrix* $M(F) \in \mathbb{C}^{s \times n}$ is defined as follows: its (i, j)th element is the coefficient $c(f_i, m_j)$ of the polynomial $f_i \in F$ at the monomial $m_j \in U_F$. Thus,

$$M(F)\,\mathbf{v}(U_F) = \mathbf{0} \tag{4}$$

is the vector form of the system of polynomial equations $f_1 = \ldots = f_s = 0$. In the following we will refer to such a system as $F = 0$ for short.

A *shift* of a polynomial f is a multiple of f by a monomial $m \in U$. Let $A = (A_1, \ldots, A_s)$ be an ordered s-tuple of finite sets of monomials $A_j \subset U$ for all j. We define the *set of shifts* of F as

$$A \cdot F = \{m \cdot f_j \; : \; \forall m \in A_j, \forall f_j \in F\}. \tag{5}$$

Let a be a Laurent monomial ($a = \frac{m_1}{m_2}$, where $m_1, m_2 \in U$ and $a \neq 1$) and $\mathcal{B}$ be a finite subset of monomials from $U_{A \cdot F}$ such that $am \in U_{A \cdot F}$ for each $m \in \mathcal{B}$. The subset $\mathcal{B}$ is called the set of *basic* monomials. The subsets

$$\mathcal{R} = \{am \; : \; m \in \mathcal{B}\} \setminus \mathcal{B} \quad \text{and} \quad \mathcal{E} = U_{A \cdot F} \setminus (\mathcal{R} \cup \mathcal{B}) \tag{6}$$

are called the sets of *reducible* and *excessive* monomials, respectively [3]. Clearly, these subsets are pairwise disjoint and $U_{A \cdot F} = \mathcal{E} \cup \mathcal{R} \cup \mathcal{B}$.

A Macaulay matrix $M(A \cdot F)$ with columns arranged in ordered blocks $M(A \cdot F) = \begin{bmatrix} M_{\mathcal{E}} & M_{\mathcal{R}} & M_{\mathcal{B}} \end{bmatrix}$ is called the *elimination template* for F with respect to a if the reduced row echelon form of $M(A \cdot F)$, denoted by $\widetilde{M}(A \cdot F)$, has the form

$$\widetilde{M}(A \cdot F) = \begin{bmatrix} \mathcal{E} & \mathcal{R} & \mathcal{B} \\ * & 0 & * \\ 0 & I & \widetilde{M}_{\mathcal{B}} \\ 0 & 0 & 0 \end{bmatrix}, \tag{7}$$

where $*$ means a submatrix with arbitrary entries, 0 is the zero matrix of a suitable size, I is the identity matrix of order $\#\mathcal{R}$ and $\widetilde{M}_{\mathcal{B}}$ is a matrix of size $\#\mathcal{R} \times \#\mathcal{B}$.

The elimination template is uniquely determined (up to reordering the rows and columns in the blocks $M_{\mathcal{E}}$, $M_{\mathcal{R}}$, $M_{\mathcal{B}}$) by the following data:

- the *action* Laurent monomial a;

- the s-tuple of sets A;

- the set of basic monomials $\mathcal{B}$.

Knowing the elimination template transforms the root-finding problem for the 0-dimensional polynomial system $F = 0$ into a computationally tractable generalized eigenvalue problem for a pair of square matrices of order $\#\mathcal{B}$. We will see in Section 4 how this works for the SGP forward kinematics problem.

An elimination template can be systematically constructed from a Gröbner basis of the polynomial ideal $\langle F \rangle$ with respect to a certain monomial ordering. In this case, $\mathcal{B}$ represents the standard linear basis of the quotient ring $\mathbb{C}[X]/\langle F \rangle$ and $\#\mathcal{B}$ equals the number of roots (with multiplicities) of the 0-dimensional system $F = 0$ [5]. Such an approach has been realized in the automatic template generators of [19, 20, 21, 26]. However, Gröbner bases are not the only way to construct elimination templates. Recent advances have developed alternative heuristic procedures [21, 1, 25]. In this case, $\mathcal{B}$ is not necessarily standard, nor is it necessarily a basis of the quotient ring. For many hard polynomial systems, these heuristic approaches frequently outperform the Gröbner-based method in template size reduction.

3. Problem statement

Consider a general Stewart–Gough platform, see Figure 1. Let $(R, \mathbf{t}) \in \mathrm{SE}(3)$ be a rigid-body transformation that relates the coordinate frames associated with the base and top platforms. Let $\mathbf{x}_i \in \mathbb{R}^3$ and $\mathbf{X}_i \in \mathbb{R}^3$ denote the positions of the ith attachment point on the top and base platforms, respectively, expressed in their local frames. Let $L_i = l_i^2$,

where l_i is the length of the ith connecting leg. Then, for each $i = 1, \dots, 6$, the fixed-distance condition for the ith leg yields

$$\| R\mathbf{x}_i + \mathbf{t} - \mathbf{X}_i \|^2 - L_i = 0, \tag{8}$$

where $\| \cdot \|$ is the Euclidean (Frobenius) norm.

Let the rotation matrix R be parametrized by the Cayley transform

$$R = (I - [\mathbf{p}]_\times)(I + [\mathbf{p}]_\times)^{-1}, \tag{9}$$

where I is the 3×3 identity matrix, $\mathbf{p} \in \mathbb{R}^3$ is the parameter vector, and $[\mathbf{p}]_\times$ denotes the skew-symmetric matrix such that $[\mathbf{p}]_\times \mathbf{q} = \mathbf{p} \times \mathbf{q}$ for any $\mathbf{q} \in \mathbb{R}^3$. Substituting (9) into Eq. (8) and clearing denominators yields a system of polynomial equations. The set of the related polynomials is denoted by $F = \{f_1, \dots, f_6\}$.

The polynomial system $F = 0$ is generically 0-dimensional, admitting exactly 40 complex roots in accordance with the well-known result that the maximum number of solutions (whether complex or real) to the forward kinematics of a general SGP is 40 [35, 22, 30, 43]. Notably, there exist special instances of F where all 40 solutions are real, distinct, and well separated [7].

Through a proper choice of coordinate frames (setting $\mathbf{x}_1 = \mathbf{X}_1 = \mathbf{0}$), the first polynomial in F simplifies to

$$f_1 = \| \mathbf{t} \|^2 - L_1. \tag{10}$$

Thus, for each particular values of

$$\begin{aligned} &\mathbf{x}_i, \mathbf{X}_i, & i = 2, \dots, 6, \\ &L_i, & i = 1, \dots, 6, \end{aligned} \tag{11}$$

the problem is to solve for $(\mathbf{p}, \mathbf{t}) \in \mathbb{R}^3 \times \mathbb{R}^3$ satisfying the six polynomial equations $F = 0$. The first quadratic equation is purely translation-dependent, while the remaining five quartic equations couple both rotation and translation parameters.

4. Description of the algorithm

In this paper we propose to solve the system $F = 0$ by the method of elimination templates. We applied state-of-the-art publicly available automatic template generators from [19, 20, 26, 25] to F. While the generators from [19, 20, 26] failed to construct a template in a reasonable time, the generator from [25] successfully constructed a template of size 293×362. To ensure reproducibility, the complete template construction data is provided in the Appendix. Here we report only the cardinalities of

- the monomial shift sets: $\#A_1 = 218, \#A_2 = 61, \#A_3 = 60, \#A_4 = 59, \#A_5 = 57, \#A_6 = 56$;

- the set of basic monomials: $\#\mathcal{B} = 69$.

The proposed algorithm consists of three main steps: 1) Template construction; 2) PLU decomposition; 3) QZ decomposition. Each step is detailed below.

4.1. Template construction
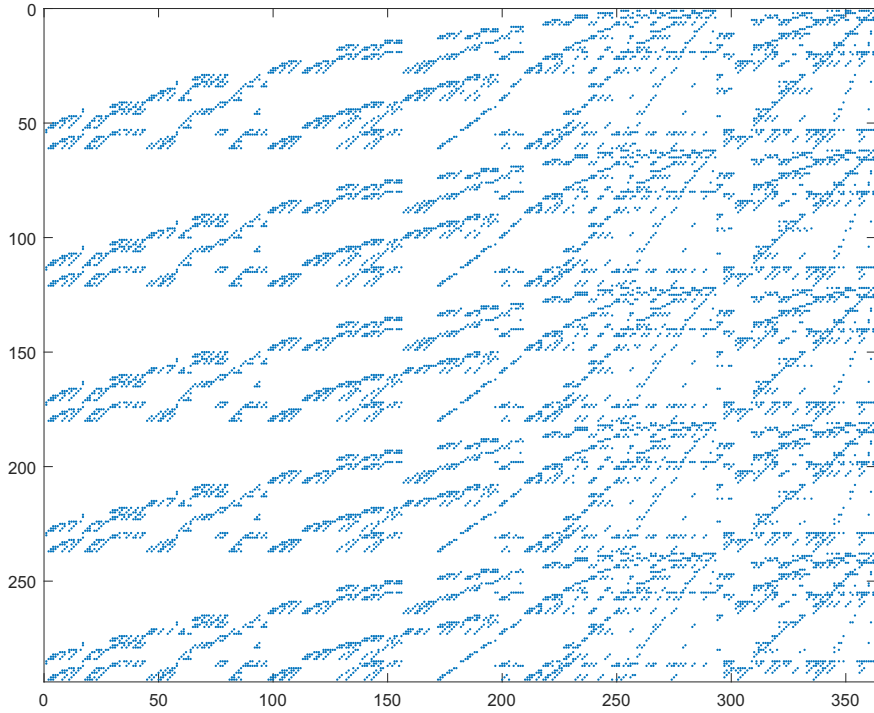
The set of shifts of F, denoted by $A \cdot F$, is constructed according to Eq. (5), where $A = (A_1, \dots, A_6)$ is the 6-tuple of monomial shift sets. This yields an initial Macaulay matrix (elimination template) of size 511×580 with the block structure

$$M(A \cdot F) = \begin{pmatrix} M_{11} & M_{12} \\ M_{21} & M_{22} \end{pmatrix}, \tag{12}$$

where the submatrix $\begin{pmatrix} M_{11} & M_{12} \end{pmatrix}$ encodes the 218 shifts of f_1. By Schur complement reduction, the template $M(A \cdot F)$ is reduced to the following template of size 293×362:

$$\widehat{M} = M_{22} - M_{21} M_0, \tag{13}$$

where $M_0 = M_{11}^{-1} M_{12}$. The matrix M_0 can be safely precomputed offline due to the special sparse form (10) of f_1. The resulting template $\widehat{M}$, visualized in Figure 2, has a sparsity of 90%.

Figure 2: Sparse pattern of the elimination template $\widehat{M}$: blue dots represent non-zero elements

4.2. PLU decomposition

The cardinalities of the sets of basic, reducible, and excessive monomials are $\#\mathcal{B} = 69$, $\#\mathcal{R} = 38$, and $\#\mathcal{E} = 255$ respectively. The monomials in vector $\mathbf{v}(\mathcal{B})$ are ordered so that its last 7 elements are

$$(\mathbf{p})_1(\mathbf{p})_3, \quad (\mathbf{p})_2(\mathbf{p})_3, \quad (\mathbf{p})_3^2, \quad (\mathbf{t})_1(\mathbf{p})_3, \quad (\mathbf{t})_2(\mathbf{p})_3, \quad (\mathbf{t})_3(\mathbf{p})_3, \quad (\mathbf{p})_3, \tag{14}$$

where $(\mathbf{p})_i$ denotes the ith entry of vector $\mathbf{p}$. The template $\widehat{M}$ has the block structure $\widehat{M} = \begin{bmatrix} \widehat{M}_{\mathcal{E}} & \widehat{M}_{\mathcal{R}} & \widehat{M}_{\mathcal{B}} \end{bmatrix}$, where $\widehat{M}_{\mathcal{E}}$ is a 293×255 sparse matrix. Performing LU decomposition with partial pivoting on $\widehat{M}_{\mathcal{E}}$ yields $\widehat{M}_{\mathcal{E}} = PLU$, where P is a permutation matrix. Then we have

$$(PL)^{-1}\widehat{M} = \begin{bmatrix} * & * & * \\ 0 & A_{\mathcal{R}} & A_{\mathcal{B}} \end{bmatrix}, \tag{15}$$

where $A_{\mathcal{R}}$ is a full-rank 38×38 matrix and $A_{\mathcal{B}}$ is a 38×69 matrix.

4.3. QZ decomposition

It follows from (15) that $A_{\mathcal{R}}\mathbf{v}(\mathcal{R}) = -A_{\mathcal{B}}\mathbf{v}(\mathcal{B})$, which translates into the following generalized eigenvalue problem:

$$aT_1\mathbf{v}(\mathcal{B}) = T_0\mathbf{v}(\mathcal{B}), \tag{16}$$

where $a = \frac{1}{(\mathbf{p})_3}$ is the action Laurent monomial. The 69×69 matrices T_0 and T_1 are constructed from $A_{\mathcal{R}}$ and $A_{\mathcal{B}}$ as follows. Let b_i be the ith element of $\mathbf{v}(\mathcal{B})$ and r_j be the jth element of $\mathbf{v}(\mathcal{R})$.

- If $ab_i = r_j$, then

  - $(T_0)_{i,k} = -(A_{\mathcal{B}})_{j,k}$ for all k;
  - $(T_1)_{i,k} = (A_{\mathcal{R}})_{j,l}$ for all pairs (k,l) such that $ab_k = r_l$.

- If $ab_i = b_j$, then

  – $(T_0)_{i,j} = 1$;

  – $(T_1)_{i,i} = 1$.

All other entries of matrices T_0 and T_1 are zero.

The numerically backward stable QZ (generalized Schur) decomposition algorithm [8, 18] is used to compute the generalized eigenvectors of the matrix pair (T_0, T_1). Let $\mathbf{u}_i$ denote the ith generalized eigenvector, with $(\mathbf{u}_i)_k$ representing its kth element. Then, according to (14), the ith solution to $F = 0$ is given by

$$\mathbf{p}_{e,i} = \frac{1}{(\mathbf{u}_i)_{69}} \begin{bmatrix} (\mathbf{u}_i)_{63} \\ (\mathbf{u}_i)_{64} \\ (\mathbf{u}_i)_{65} \end{bmatrix}, \quad \mathbf{t}_{e,i} = \frac{1}{(\mathbf{u}_i)_{69}} \begin{bmatrix} (\mathbf{u}_i)_{66} \\ (\mathbf{u}_i)_{67} \\ (\mathbf{u}_i)_{68} \end{bmatrix}. \tag{17}$$

The corresponding rotation matrix $R_{e,i}$ is obtained from $\mathbf{p}_{e,i}$ via the Cayley transform (9).

The proposed algorithm outputs $69 - 40 = 29$ false roots that need to be filtered out by back substitution. Let the polynomial system $F = 0$ be written in the form $M(F)\mathbf{z} = \mathbf{0}$, where $M(F)$ and $\mathbf{z} = \mathbf{v}(U_F)$ are the normalized Macaulay matrix (with unit row norms) and monomial vector respectively. Let $\mathbf{z}_i$ be the monomial vector $\mathbf{z}$ evaluated at the ith (possibly false) root. We compute the residuals

$$\epsilon_i = \left\| M(F) \frac{\mathbf{z}_i}{\|\mathbf{z}_i\|} \right\| \tag{18}$$

and sort them in ascending order. Then the true roots correspond to the first 40 values of ϵ_i.

5. Experiments

The algorithm has been implemented in MATLAB, Julia, and Python. The experiments were conducted on an Intel Core i5-1155G7 processor using the MATLAB implementation. For all the tests, $\mathbf{x}_1 = \mathbf{X}_1 = \mathbf{0}$ and $\mathbf{x}_i, \mathbf{X}_i$ ($i = 2, \ldots, 6$) are uniformly distributed random 3-vectors from $[-2, 2]^{\times 3}$.

While our primary focus is the general 6-6 SGP, the solver also handles two special cases:

- 6-5: two attachment points on the top platform coincide;

- 6P-6: semi-planar case (all base attachment points lie in a plane).

Remark 1. Since the kinematic equations (8) are invariant under the transformations $\mathbf{x}_i \leftrightarrow \mathbf{X}_i$, $R \to R^{\mathsf{T}}$, $\mathbf{t} \to -R^{\mathsf{T}}\mathbf{t}$, where the superscript T indicates matrix transpose, the configurations 5-6 and 6-6P are equivalent to 6-5 and 6P-6 respectively.

Remark 2. While the fully planar 6P-6P configuration is a degenerate case for the proposed solver, experiments confirm that the solver is able to handle the "almost planar" case, where only one point on the top or base platform is outside the plane.
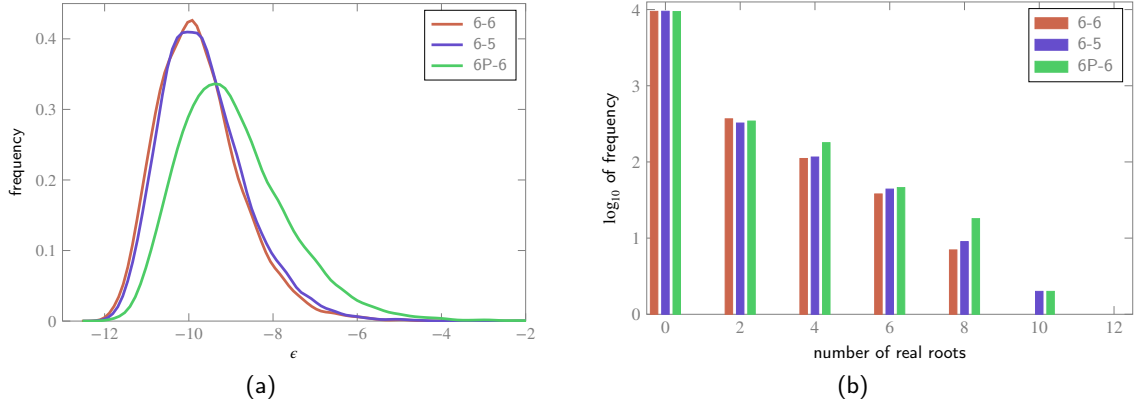
5.1. Numerical accuracy, number of real roots, and speed

For this test, each squared leg length L_i was sampled independently from a uniform distribution over the interval $[0.5, 3]$. The numerical accuracy is quantified by computing the error metric

$$\epsilon = \frac{1}{2} \log_{10} \sum_{i=1}^{40} \epsilon_i^2, \tag{19}$$

where the residuals ϵ_i are defined in Eq. (18). Figure 3(a) shows the error distribution histograms, while Table 1 provides detailed statistics including the median, mean, and maximum values of ϵ over all trials.

Figure 3(b) shows the distribution of real root counts using a logarithmic y-axis for better visualization. The results reveal that approximately 95% of trials produce no real roots, while the remaining trials produce between 2 and 10 real roots. Although the general 6-6 configuration is known to admit a maximum of 40 real roots [7], the maximum number

Figure 3: Distributions over 10^4 trials: (a) numerical errors, (b) real root counts (logarithmic y-axis scale)

SGP type	Med. ϵ	Mean ϵ	Max. ϵ	$\epsilon > -5$	$\epsilon > -6$	Med. $(\epsilon_{40} - \epsilon_{41})$	Mean $(\epsilon_{40} - \epsilon_{41})$
6-6	-9.86	-9.71	-3.41	0.13%	0.38%	-8.69	-8.56
6-5	-9.76	-9.63	-1.34	0.15%	0.46%	-8.48	-8.36
6P-6	-9.12	-8.94	-0.71	0.91%	2.71%	-7.78	-7.61

Table 1
Complementary to Figure 3(a). Columns 2–6: error distribution statistics, columns 7–8: true/false roots boundary sharpness statistics

Step	Template	PLU	QZ	Total
Time (ms)	0.4	4.2	1.6	6.2

Table 2
Average runtime across the main steps of the algorithm

of real roots for both 6-5 and 6P-6 configurations is currently unknown (to the best of the author's knowledge). The observed maximum over more than 10^5 trials was 12 for both special cases.

Table 2 summarizes the average runtime distribution across the three main steps of the algorithm: 1) construction of the elimination template $\widehat{M}$, see Eq. (13); 2) PLU decomposition of the 293×255 sparse matrix $\widehat{M}_{\mathcal{E}}$ followed by matrix division in Eq. (15); 3) QZ decomposition of the matrix pair (T_0, T_1). It can be seen that most of the time ($> 67\%$) is spent on step 2. Leveraging the specific sparse pattern of the matrix $\widehat{M}$, as shown in Figure 2, could potentially lead to enhanced efficiency in the PLU decomposition step.

5.2. Behaviour under uncertainties

In this subsection we demonstrate that the solver maintains continuous dependence on input parameters — small measurement errors produce small deviations in the estimated rigid-body transformation. This stability property ensures predictable behaviour in real-world applications.

For this test, each squared leg length L_i was computed from Eq. (8) using standard normally distributed translation ($\mathbf{t}$) and rotation ($\mathbf{p}$) vectors. To simulate measurement uncertainty, each squared length was perturbed as $L_i(1 + s_i)^2$, where s_i has a normal distribution with zero mean and standard deviation σ ranging from 0 to 8×10^{-4}.
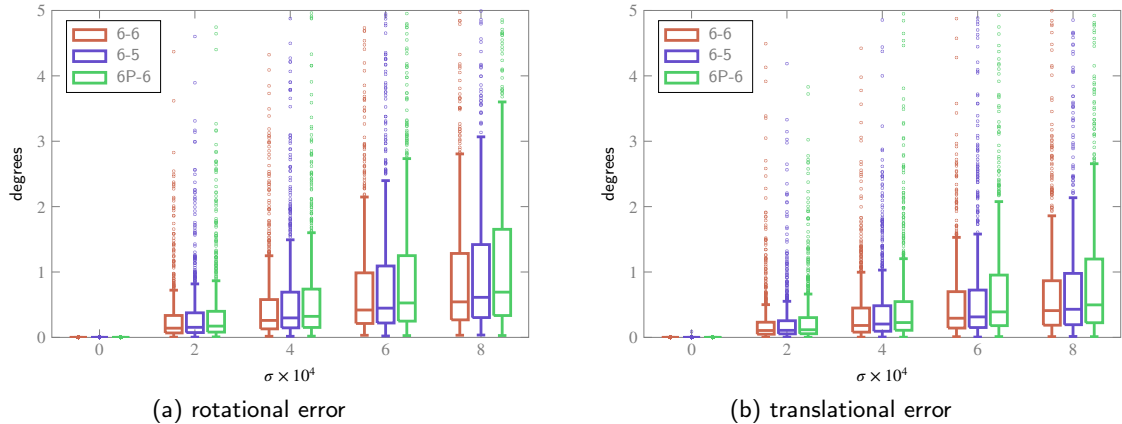
To evaluate solver accuracy, we compared the estimated rigid-body transformations to the ground truth by computing the rotational and translational errors:

$$\epsilon_R = \min_i \arccos \frac{\mathrm{tr}(R_{\mathrm{e},i}^{\top} R_{\mathrm{gt}}) - 1}{2}, \tag{20}$$

$$\epsilon_{\mathbf{t}} = \min_i \arccos \frac{\mathbf{t}_{\mathrm{e},i}^{\top} \mathbf{t}_{\mathrm{gt}}}{\|\mathbf{t}_{\mathrm{e},i}\| \, \|\mathbf{t}_{\mathrm{gt}}\|}. \qquad (21)$$

Here, $\mathrm{tr}(\cdot)$ is the trace function, $(R_{\mathrm{gt}}, \mathbf{t}_{\mathrm{gt}})$ is the ground truth transformation, $(R_{\mathrm{e},i}, \mathbf{t}_{\mathrm{e},i})$ is the ith estimated transformation, and the minimum is taken over all real solutions.

Figure 4 demonstrates the behaviour of the solver as σ increases. Each boxplot displays the data distribution with the lower (25%) and upper (75%) quartiles forming the box, the median marked by an internal line, and whiskers extending to data points within 1.5× the interquartile range. Outliers beyond the whiskers are represented by individual dots. The results confirm the predictable solver behaviour for all three SGP types, although the results are slightly worse for the semi-planar case. Under noise-free conditions ($\sigma = 0$), both rotational and translational errors vanish with no outliers observed.

(a) rotational error　　　　　　　　　　　(b) translational error

Figure 4: Rotational and translational errors against the level of leg length measurement uncertainty. Each boxplot summarizes the results from 10^3 independent trials

6. Conclusion

This paper proposes a novel practical algorithm for solving the forward kinematics problem for a general Stewart—Gough platform. The proposed algorithm is purely algebraic, requiring no geometric assumptions about the base or top platforms and no additional sensor data. All 40 solutions to the problem (real and complex) are derived from the generalized eigenvectors of a pair of 69×69 matrices.

A series of experiments on synthetic data validate the algorithm's numerical accuracy and predictable behaviour under measurement uncertainty in leg lengths. With an average runtime of approximately 6ms on standard hardware, the solver is compatible with real-time control for some applications.

Finally, while this paper addresses the general 6-6 SGP configuration along with the 6-5 and 6P-6 special cases, the method of elimination templates provides a general framework for developing efficient solvers for other common types of SGPs, including 6-4, 6-3, 5-5, 5-4, etc.

A. Data for template construction

This appendix provides the data needed to construct the elimination template found by the automatic generator from [25]. Let $\mathbf{p} = \begin{bmatrix} u & v & w \end{bmatrix}^{\top}$ and $\mathbf{t} = \begin{bmatrix} x & y & z \end{bmatrix}^{\top}$, see Section 3 for description. Then

- the action Laurent monomial: $a = \frac{1}{w}$;

- the monomial shift sets:

$$
\begin{aligned}
A_1 = \{ & 1, \quad z, \quad y, \quad x, \quad w, \quad v, \quad u, \quad z^2, \quad yz, \quad xz, \quad zw, \quad vz, \\
& uz, \quad y^2, \quad xy, \quad wy, \quad vy, \quad uy, \quad x^2, \quad wx, \quad vx, \quad ux, \quad w^2, \quad vw, \\
& uw, \quad v^2, \quad uv, \quad u^2, \quad zwy, \quad yvz, \quad yuz, \quad zwx, \quad xvz, \quad zxu, \quad zw^2, \quad zv^2, \\
& zvu, \quad zu^2, \quad y^2w, \quad y^2v, \quad y^2u, \quad yxw, \quad yxv, \quad yxu, \quad yw^2, \quad ywu, \quad yv^2, \quad yvu, \\
& yu^2, \quad wx^2, \quad vx^2, \quad ux^2, \quad xw^2, \quad xwv, \quad xwu, \quad xv^2, \quad xvu, \quad xu^2, \quad w^3, \quad w^2v, \\
& w^2u, \quad wv^2, \quad wvu, \quad wu^2, \quad v^3, \quad v^2u, \quad vu^2, \quad u^3, \quad w^2z^2, \quad v^2z^2, \quad u^2z^2, \quad yzw^2, \\
& yzv^2, \quad yzu^2, \quad xzw^2, \quad xzv^2, \quad xzu^2, \quad w^3z, \quad vzw^2, \quad uzw^2, \quad v^2zw, \quad u^2zw, \quad v^3z, \quad uzv^2, \\
& vzu^2, \quad u^3z, \quad w^2y^2, \quad v^2y^2, \quad u^2y^2, \quad xyw^2, \quad xyv^2, \quad xyu^2, \quad w^3y, \quad vyw^2, \quad uyw^2, \quad v^2yw, \\
& wyu^2, \quad v^3y, \quad uyv^2, \quad u^2yv, \quad u^3y, \quad w^2x^2, \quad v^2x^2, \quad u^2x^2, \quad w^3x, \quad vxw^2, \quad uxw^2, \quad wxv^2, \\
& u^2xw, \quad v^3x, \quad uxv^2, \quad u^2xv, \quad u^3x, \quad w^4, \quad w^3v, \quad w^3u, \quad w^2v^2, \quad w^2uv, \quad w^2u^2, \quad v^3w, \\
& v^2uw, \quad vu^2w, \quad u^3w, \quad v^4, \quad v^3u, \quad v^2u^2, \quad u^3v, \quad u^4, \quad zw^3y, \quad zvyw^2, \quad zuyw^2, \quad zv^2yw, \\
& zwyu^2, \quad zv^3y, \quad zuyv^2, \quad zu^2yv, \quad zu^3y, \quad zw^3x, \quad zvxw^2, \quad zuxw^2, \quad zwxv^2, \quad zu^2xw, \quad zv^3x, \quad zuxv^2, \\
& zu^2xv, \quad zu^3x, \quad w^4z, \quad vw^3z, \quad uw^3z, \quad v^2w^2z, \quad uvw^2z, \quad u^2w^2z, \quad v^3wz, \quad uv^2wz, \quad u^2vwz, \quad u^3wz, \\
& v^4z, \quad uv^3z, \quad u^2v^2z, \quad u^3vz, \quad u^4z, \quad w^3y^2, \quad vw^2y^2, \quad uw^2y^2, \quad wv^2y^2, \quad wu^2y^2, \quad v^3y^2, \quad uv^2y^2, \\
& vu^2y^2, \quad u^3y^2, \quad w^3xy, \quad vw^2xy, \quad uw^2xy, \quad v^2wxy, \quad u^2wxy, \quad v^3xy, \quad uv^2xy, \quad u^2vxy, \quad u^3xy, \quad w^4y, \\
& vw^3y, \quad uw^3y, \quad v^2w^2y, \quad uvw^2y, \quad u^2w^2y, \quad v^3wy, \quad uv^2wy, \quad u^2vwy, \quad u^3wy, \quad v^4y, \quad uv^3y, \quad u^2v^2y, \\
& u^3vy, \quad u^4y, \quad w^3x^2, \quad vw^2x^2, \quad uw^2x^2, \quad wv^2x^2, \quad wu^2x^2, \quad v^3x^2, \quad uv^2x^2, \quad vu^2x^2, \quad u^3x^2, \quad w^4x, \\
& vw^3x, \quad uw^3x, \quad v^2w^2x, \quad uvw^2x, \quad u^2w^2x, \quad v^3wx, \quad uv^2wx, \quad u^2vwx, \quad u^3wx, \quad v^4x, \quad uv^3x, \quad u^2v^2x, \\
& u^3vx, \quad u^4x \},
\end{aligned}
$$

$$
\begin{aligned}
A_2 = \{ & 1, \quad z, \quad y, \quad x, \quad w, \quad v, \quad u, \quad z^2, \quad yz, \quad xz, \quad zw, \quad vz, \quad uz, \quad y^2, \quad xy, \\
& wy, \quad vy, \quad uy, \quad x^2, \quad wx, \quad vx, \quad ux, \quad w^2, \quad vw, \quad uw, \quad v^2, \quad uv, \quad u^2, \quad zwy, \quad yvz, \\
& yuz, \quad zwx, \quad xvz, \quad zxu, \quad zw^2, \quad zwv, \quad zwu, \quad zv^2, \quad zvu, \quad zu^2, \quad y^2w, \quad y^2v, \quad y^2u, \quad yxw, \quad yxv, \\
& yxu, \quad yw^2, \quad ywv, \quad ywu, \quad yv^2, \quad yvu, \quad yu^2, \quad wx^2, \quad vx^2, \quad ux^2, \quad xw^2, \quad xwv, \quad xwu, \quad xv^2, \quad xvu, \\
& xu^2 \},
\end{aligned}
$$

$$
\begin{aligned}
A_3 = \{ & 1, \quad z, \quad y, \quad x, \quad w, \quad v, \quad u, \quad z^2, \quad yz, \quad xz, \quad zw, \quad vz, \quad uz, \quad y^2, \quad xy, \\
& wy, \quad vy, \quad uy, \quad x^2, \quad wx, \quad vx, \quad ux, \quad w^2, \quad vw, \quad uw, \quad v^2, \quad uv, \quad u^2, \quad zwy, \quad yvz, \\
& yuz, \quad zwx, \quad xvz, \quad zxu, \quad zw^2, \quad zwu, \quad zv^2, \quad zvu, \quad zu^2, \quad y^2w, \quad y^2v, \quad y^2u, \quad yxw, \quad yxv, \quad yxu, \\
& yw^2, \quad ywv, \quad ywu, \quad yv^2, \quad yvu, \quad yu^2, \quad wx^2, \quad vx^2, \quad ux^2, \quad xw^2, \quad xwv, \quad xwu, \quad xv^2, \quad xvu, \quad xu^2 \},
\end{aligned}
$$

$$
\begin{aligned}
A_4 = \{ & 1, \quad z, \quad y, \quad x, \quad w, \quad v, \quad u, \quad z^2, \quad yz, \quad xz, \quad zw, \quad vz, \quad uz, \quad y^2, \quad xy, \\
& wy, \quad vy, \quad uy, \quad x^2, \quad wx, \quad vx, \quad ux, \quad w^2, \quad vw, \quad uw, \quad v^2, \quad uv, \quad u^2, \quad zwy, \quad yvz, \\
& yuz, \quad zwx, \quad xvz, \quad zxu, \quad zw^2, \quad zv^2, \quad zvu, \quad zu^2, \quad y^2w, \quad y^2v, \quad y^2u, \quad yxw, \quad yxv, \quad yxu, \quad yw^2, \\
& ywv, \quad ywu, \quad yv^2, \quad yvu, \quad yu^2, \quad wx^2, \quad vx^2, \quad ux^2, \quad xw^2, \quad xwv, \quad xwu, \quad xv^2, \quad xvu, \quad xu^2 \},
\end{aligned}
$$

$$
\begin{aligned}
A_5 = \{ & 1, \quad z, \quad y, \quad x, \quad w, \quad v, \quad u, \quad yz, \quad xz, \quad zw, \quad vz, \quad uz, \quad y^2, \quad xy, \quad wy, \\
& vy, \quad uy, \quad x^2, \quad wx, \quad vx, \quad ux, \quad w^2, \quad vw, \quad uw, \quad v^2, \quad uv, \quad u^2, \quad zwy, \quad yvz, \quad yuz, \\
& zwx, \quad xvz, \quad zxu, \quad zw^2, \quad zv^2, \quad zvu, \quad zu^2, \quad y^2w, \quad y^2v, \quad y^2u, \quad yxw, \quad yxv, \quad yxu, \quad yw^2, \quad ywu, \\
& yv^2, \quad yvu, \quad yu^2, \quad wx^2, \quad vx^2, \quad ux^2, \quad xw^2, \quad xwv, \quad xwu, \quad xv^2, \quad xvu, \quad xu^2 \},
\end{aligned}
$$

$$
\begin{aligned}
A_6 = \{ & 1, \quad z, \quad y, \quad x, \quad w, \quad v, \quad u, \quad yz, \quad xz, \quad zw, \quad vz, \quad uz, \quad y^2, \quad xy, \quad wy, \\
& vy, \quad uy, \quad x^2, \quad wx, \quad vx, \quad ux, \quad w^2, \quad vw, \quad uw, \quad v^2, \quad uv, \quad u^2, \quad zwy, \quad yvz, \quad yuz, \\
& zwx, \quad xvz, \quad zxu, \quad zv^2, \quad zvu, \quad zu^2, \quad y^2w, \quad y^2v, \quad y^2u, \quad yxw, \quad yxv, \quad yxu, \quad yw^2, \quad ywu, \quad yv^2, \\
& yvu, \quad yu^2, \quad wx^2, \quad vx^2, \quad ux^2, \quad xw^2, \quad xwv, \quad xwu, \quad xv^2, \quad xvu, \quad xu^2 \};
\end{aligned}
$$

- the set of basic monomials:

$$
\begin{aligned}
\mathcal{B} = \{ & zuyw^2, \quad zvyw^2, \quad zw^3y, \quad z^2uwv, \quad wv^2z^2, \quad uw^2z^2, \quad vw^2z^2, \quad w^3z^2, \quad v^3w, \quad w^2u^2, \quad w^2uv, \quad w^2v^2, \\
& w^3u, \quad w^3v, \quad w^4, \quad w^3x, \quad uywv, \quad v^2yw, \quad uyw^2, \quad vyw^2, \quad w^3y, \quad yxwu, \quad xywv, \quad xyw^2, \\
& uwy^2, \quad y^2wv, \quad w^2y^2, \quad u^2zw, \quad uzwv, \quad v^2zw, \quad uzw^2, \quad vzw^2, \quad w^3z, \quad xzwu, \quad xzwv, \quad xzw^2, \\
& yzwu, \quad yzwv, \quad yzw^2, \quad z^2wu, \quad z^2wv, \quad w^2z^2, \quad wu^2, \quad wvu, \quad wv^2, \quad w^2u, \quad w^2v, \quad w^3, \\
& xwu, \quad xwv, \quad xw^2, \quad ywu, \quad ywv, \quad yw^2, \quad yxw, \quad wy^2, \quad zwu, \quad zwv, \quad zw^2, \quad zwx, \\
& zwy, \quad wz^2, \quad wu, \quad vw, \quad w^2, \quad xw, \quad yw, \quad zw, \quad w \}.
\end{aligned}
$$

CRediT authorship contribution statement

Martyushev: Conceptualization, Methodology, Software, Validation, Visualization, Writing.

Declaration of competing interest

The author declares that he has no known competing financial interests or personal relationships that could appear to influence the work in this paper.

Data availability

Reference implementations of the proposed algorithm in MATLAB, Julia, and Python are available under an open-source license at https://github.com/martyushev/fkSGP.

References

[1] Bhayani, S., Kukelova, Z., Heikkila, J., 2020. A sparse resultant based method for efficient minimal solvers, in: Proceedings of the IEEE/CVF Conference on Computer Vision and Pattern Recognition, pp. 1770–1779.

[2] Boudreau, R., Turkkan, N., 1996. Solving the forward kinematics of parallel manipulators with a genetic algorithm. Journal of Robotic Systems 13, 111–125.

[3] Byröd, M., Josephson, K., Åström, K., 2009. Fast and stable polynomial equation solving and its application to computer vision. International Journal of Computer Vision 84, 237–256.

[4] Chauhan, D.K.S., Vundavilli, P.R., 2022. Forward kinematics of the Stewart parallel manipulator using machine learning. International Journal of Computational Methods 19, 2142009.

[5] Cox, D.A., Little, J., O'Shea, D., 2015. Ideals, Varieties, and Algorithms: An Introduction to Computational Algebraic Geometry and Commutative Algebra. Springer.

[6] Didrit, O., Petitot, M., Walter, E., 1998. Guaranteed solution of direct kinematic problems for general configurations of parallel manipulators. IEEE Transactions on Robotics and Automation 14, 259–266.

[7] Dietmaier, P., 1998. The Stewart-Gough platform of general geometry can have 40 real postures, in: Advances in robot kinematics: Analysis and control. Springer, pp. 7–16.

[8] Golub, G.H., Van Loan, C.F., 2013. Matrix computations. JHU press.

[9] Gough, V.E., 1962. Universal tyre test machine. Proc. FISITA 9th Int. Technical Congr., London, 1962 , 117–137.

[10] Griffis, M., Duffy, J., 1989. A forward displacement analysis of a class of Stewart platforms. Journal of Robotic Systems 6, 703–720.

[11] Grishin, N., Bukharov, K., Rybak, L., Zhuk, V., 2023. Numerical method for solving the forward kinematics to control the Gough-Stewart platform, in: AIP Conference Proceedings, AIP Publishing.

[12] Huang, X., He, G., 2009. Forward kinematics of the general Stewart-Gough platform using Gröbner basis, in: 2009 International Conference on Mechatronics and Automation, IEEE. pp. 3557–3561.

[13] Huang, X., Liao, Q., Wei, S., Qiang, X., Huang, S., 2007. Forward kinematics of the 6-6 Stewart platform with planar base and platform using algebraic elimination, in: 2007 IEEE International Conference on Automation and Logistics, IEEE. pp. 2655–2659.

[14] Husty, M.L., 1996. An algorithm for solving the direct kinematics of general Stewart-Gough platforms. Mechanism and Machine Theory 31, 365–379.

[15] Innocenti, C., Parenti-Castelli, V., 1990. Direct position analysis of the Stewart platform mechanism. Mechanism and Machine Theory 25, 611–621.

[16] Ji, P., Wu, H., 2001. A closed-form forward kinematics solution for the 6-6/sup p/Stewart platform. IEEE Transactions on Robotics and Automation 17, 522–526.

[17] Karmakar, S., Turner, C.J., 2024. Non-invasive calibration of a Stewart platform by photogrammetry. The International Journal of Advanced Manufacturing Technology 132, 2601–2616.

[18] Kressner, D., et al., 2005. Numerical methods for general and structured eigenvalue problems. Springer Berlin Heidelberg.

[19] Kukelova, Z., Bujnak, M., Pajdla, T., 2008. Automatic generator of minimal problem solvers, in: European Conference on Computer Vision, Springer. pp. 302–315.

[20] Larsson, V., Åström, K., Oskarsson, M., 2017. Efficient solvers for minimal problems by syzygy-based reduction, in: Proceedings of the IEEE Conference on Computer Vision and Pattern Recognition, pp. 820–829.

[21] Larsson, V., Oskarsson, M., Åström, K., Wallis, A., Kukelova, Z., Pajdla, T., 2018. Beyond Gröbner bases: Basis selection for minimal solvers, in: Proceedings of the IEEE Conference on Computer Vision and Pattern Recognition, pp. 3945–3954.

[22] Lazard, D., 1993. On the representation of rigid-body motions and its application to generalized platform manipulators. Computational Kinematics , 175–181.

[23] Lee, T.Y., Shim, J.K., 2001. Forward kinematics of the general 6–6 Stewart platform using algebraic elimination. Mechanism and Machine Theory 36, 1073–1085.

[24] Lee, T.Y., Shim, J.K., 2003. Improved dialytic elimination algorithm for the forward kinematics of the general Stewart–Gough platform. Mechanism and Machine Theory 38, 563–577.

[25] Martyushev, E., Bhayani, S., Pajdla, T., 2024. Automatic solver generator for systems of Laurent polynomial equations. preprint: https://arxiv.org/abs/2307.00320 .

[26] Martyushev, E., Vrablikova, J., Pajdla, T., 2022. Optimizing elimination templates by greedy parameter search, in: Proceedings of the IEEE/CVF Conference on Computer Vision and Pattern Recognition, pp. 15754–15764.

[27] Merlet, J.P., 2002. Direct kinematics of parallel manipulators. IEEE Transactions on Robotics and Automation 9, 842–846.

[28] Merlet, J.P., 2004. Solving the forward kinematics of a Gough-type parallel manipulator with interval analysis. The International Journal of Robotics Research 23, 221–235.

[29] Morell, A., Tarokh, M., Acosta, L., 2013. Solving the forward kinematics problem in parallel robots using Support Vector Regression. Engineering Applications of Artificial Intelligence 26, 1698–1706.

[30] Mourrain, B., 1993. The 40 "generic" positions of a parallel robot, in: Proceedings of the 1993 international symposium on Symbolic and algebraic computation, pp. 173–182.

[31] Nag, A., Safar, V., Bandyopadhyay, S., 2021. A uniform geometric-algebraic framework for the forward kinematic analysis of 6-6 Stewart platform manipulators of various architectures and other related 6-6 spatial manipulators. Mechanism and Machine Theory 155, 104090.

[32] Nielsen, J., Roth, B., 1996. The direct kinematics of the general 6–5 Stewart-Gough mechanism, in: Recent Advances in Robot Kinematics. Springer, pp. 7–16.

[33] Omran, A., Bayoumi, M., Kassem, A., El-Bayoumi, G., 2009. Optimal forward kinematics modeling of Stewart manipulator using genetic algorithms. Jordan Journal of Mechanical and Industrial Engineering 3, 280–293.

[34] Parikh, P.J., Lam, S.S., 2009. Solving the forward kinematics problem in parallel manipulators using an iterative artificial neural network strategy. The International Journal of Advanced Manufacturing Technology 40, 595–606.

[35] Raghavan, M., 1993. The Stewart platform of general geometry has 40 configurations. ASME J. of Mechanical Design 115, 277–282.

[36] Sadjadian, H., Taghirad, H.D., Fatehi, A., 2005. Neural networks approaches for computing the forward kinematics of a redundant parallel manipulator. International Journal of Computational Intelligence 2, 40–47.

[37] Safeena, M., Jiji, K., et al., 2022. Survey paper on the forward kinematics solution of a Stewart platform, in: 2022 Second International Conference on Next Generation Intelligent Systems (ICNGIS), IEEE. pp. 1–8.

[38] Schulz, S., Seibel, A., Schreiber, D., Schlattmann, J., 2017. Sensor concept for solving the direct kinematics problem of the Stewart-Gough platform, in: 2017 IEEE/RSJ International Conference on Intelligent Robots and Systems (IROS), IEEE. pp. 1959–1964.

[39] Seibel, A., Schulz, S., Schlattmann, J., 2018. On the direct kinematics problem of parallel mechanisms. Journal of Robotics 2018, 2412608.

[40] Sheng, L., Wan-long, L., Yan-chun, D., Liang, F., 2006. Forward kinematics of the Stewart platform using hybrid immune genetic algorithm, in: 2006 International Conference on Mechatronics and Automation, IEEE. pp. 2330–2335.

[41] Stewart, D., 1965. A platform with six degrees of freedom. Proceedings of the Institution of Mechanical Engineers 180, 371–386.

[42] Tarokh, M., 2007. Real time forward kinematics solutions for general Stewart platforms, in: Proceedings 2007 IEEE International Conference on Robotics and Automation, IEEE. pp. 901–906.

[43] Wampler, C.W., 1996. Forward displacement analysis of general six-in-parallel SPS (Stewart) platform manipulators using soma coordinates. Mechanism and Machine Theory 31, 331–337.

[44] Wang, Y., 2007. A direct numerical solution to forward kinematics of general Stewart–Gough platforms. Robotica 25, 121–128.

[45] Yin, Z., Qin, R., Liu, Y., 2022. A new solving method based on simulated annealing particle swarm optimization for the forward kinematic problem of the Stewart–Gough platform. Applied Sciences 12, 7657.